[6] Cell Imaging Assays for G Protein-Coupled Receptor Internalization: Application to High-Throughput Screening

By SEUNGTAEK LEE, BONNIE HOWELL, and PRIYA KUNAPULI

Abstract

There are a number of assays currently available to study G protein-coupled receptors (GPCRs), including ligand binding and functional assays. The latter category, albeit more complex, offers some obvious advantages over traditional ligand-binding assays. Functional cell-based assays typically include second messenger and reporter gene assays, which depend directly or indirectly on the cellular signaling cascade initiated upon receptor activation, respectively. More recently, cell imaging assays monitoring receptor trafficking are becoming increasingly popular. These assays, described in greater detail in this chapter, are independent of receptor signaling and are thus ideally suited for orphan receptors. In addition, these assays provide a valuable measure of receptor desensitization, an important feature for the use of GPCR agonists as potential therapeutic agents. The most popular GPCR imaging assays are based on the principles of receptor desensitization and internalization monitored directly or indirectly by green fluorescent protein.

Introduction

G protein-coupled receptors (GPCRs) constitute one of the largest families of druggable targets in the human genome (Bleicher, 2003; Drews, 2000). Not surprisingly, approximately 45% of currently available pharmaceutical drugs are targeted against this class of cell surface receptors (Bleicher *et al.*, 2003; Hopkins and Groom, 2002). The vast genomics effort has led to the identification of a number of GPCRs in the human genome, some of which remain ''orphan'' with unknown endogenous ligand and function (Civelli *et al.*, 2001; Marchese *et al.*, 1999). In this postgenomic era, a considerable research effort is aimed at deorphanizing these receptors and understanding their role in human physiology and their potential therapeutic value.

GPCRs constitute a superfamily of cell surface receptors with a common motif of seven membrane-spanning domains. Agonist stimulation initiates a cascade of signals that involve activation of the heterotrimeric GTP-binding proteins (G proteins) (Gautam *et al.*, 1998; Neer, 1995),

METHODS IN ENZYMOLOGY, VOL. 414

0076-6879/06 $35.00
DOI: 10.1016/S0076-6879(06)14006-9

resulting in second messenger-dependent modulation of various effector systems (Gilman, 1987) and feedback regulation of G protein coupling by receptor desensitization and receptor endocytosis (Krupnick and Benovic, 1998; Lefkowitz, 1993).

Functional assays to monitor the GPCR–ligand interaction are useful for overcoming some of the limitations of traditional ligand-binding assays. Commonly used functional assays for GPCRs include second messenger assays (for cAMP, IP_3, or intracellular Ca^{2+}) and reporter gene assays. More recently, the use of receptor trafficking assays is becoming increasingly popular for orphan receptors with unknown cellular signaling, as well as for the determination of receptor desensitization induced by agonists with the potential for use as therapeutic agents.

Elucidation of the mechanism of regulation of GPCR function by receptor desensitization in the 1990s laid the foundation for the receptor internalization/trafficking assay. This assay is unique in being independent of the second messenger signaling modulated by the receptor–ligand interaction. GPCR desensitization (waning of the receptor responsiveness with time) is mediated primarily by two protein families: G protein-coupled receptor kinases (GRKs) and arrestins (Ferguson, 2001). Agonist stimulation of GPCRs promotes the phosphorylation of serine/threonine residues located predominantly in the carboxyl-terminal tail and/or the third intracellular loop of the receptor by the family of GRKs. This in turn triggers the translocation of the arrestin family of proteins from the cytoplasm to the receptors at the plasma membrane. Arrestin binding to the activated and GRK-phosphorylated receptors effectively uncouples the receptor–G protein interaction, thereby terminating receptor signaling (Gurevich *et al.*, 1995).

The arrestin proteins bound to the activated and phosphorylated receptor subsequently target GPCRs for endocytosis via clathrin-coated pits (Goodman *et al.*, 1996; Krupnik *et al.*, 1997; Oakley *et al.*, 2002; Sterne-Marr and Benovic, 1995). Based on the affinity of the arrestin–GPCR interaction, receptor endocytosis results in either transient complexes of the GPCR/arrestin/clathrin-coated pits near the plasma membrane (for low-affinity interactions) or stable GPCR/arrestin complexes that internalize into intracellular vesicles (for high-affinity interactions) (Oakley *et al.*, 1999, 2000, 2001). Thus, the movement of activated GPCRs from the plasma membrane into either pits or vesicles can be monitored as an indication of receptor activation and forms the basis of a functional high-content cell-based assay (Fig. 1).

Among the different GPCR functional cell-based assays currently available, the receptor trafficking assay offers value as a receptor ''proximal'' readout (unlike the reporter gene assays) and is particularly advantageous for receptors that lack a suitable radioligand for use in receptor-binding assays. In addition, this assay can be used for most GPCRs without a priori

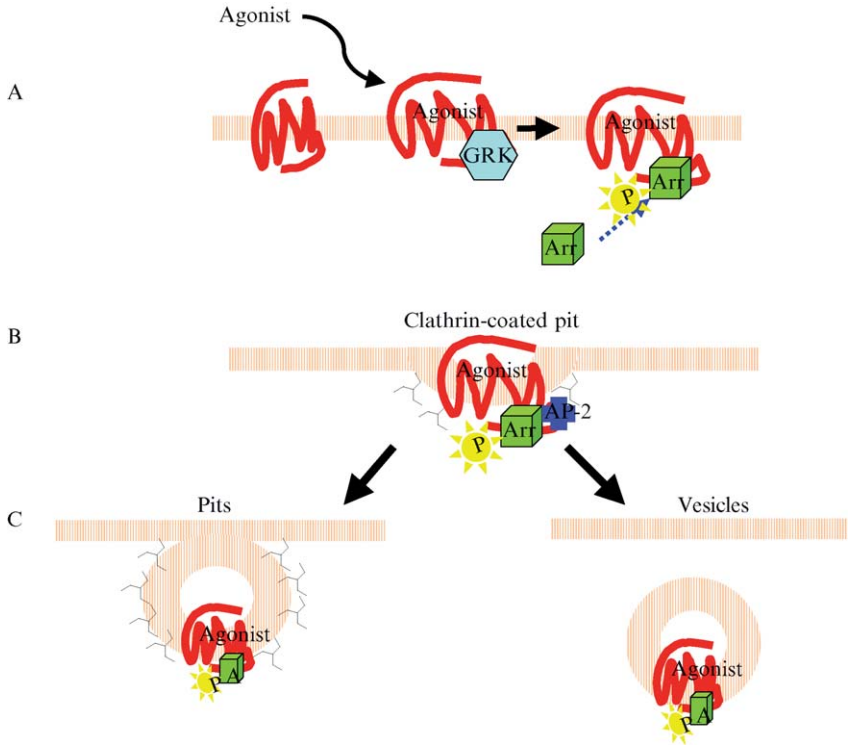

FIG. 1. Schematic representation of GPCR internalization process.

knowledge of the agonist-induced signaling cascade. Another advantage of this functional assay is the potential to identify different categories of ligands: classical competitive antagonists (also identified by the receptor-binding assay), as well as allosteric modulators (i.e., compounds that do not inhibit the binding of a radioligand to the receptor) that presumably inhibit receptor function by binding to sites on the receptor distinct from the agonist-binding pocket.

Monitoring GPCR Trafficking via Receptor–GFP

Overview

Two methods prevail to monitor GPCR trafficking in cells, both involving green fluorescent proteins (GFP). The most direct method is to express the GPCR of interest recombinantly as a chimera with GFP in the

carboxyl-terminal tail and monitor the fluorescence localization in the cell upon receptor activation.

This chapter describes internalization of the chemokine receptor CXCR3, monitored by direct fusion of GFP to the carboxyl-terminal of the receptor tail. The human CXCR3 receptor cDNA was engineered with emerald GFP at the carboxyl-terminal tail of the receptor [stop codon and emerald GFP sequence separated by Gly(5)-Ala peptide linker]. The assay was developed to confirm CXCR3 receptor antagonists from a subset of compounds originally identified as potential receptor antagonists in a reporter gene β-lactamase (BLA) assay by high-throughput screening (HTS).

Assay Protocol

The homogeneous addition only assay protocol is detailed in Fig. 2. Cell images were analyzed with the Granularity Analysis algorithm (Fig. 3).

Kinetics of Receptor Internalization

Kinetics of CXCR3-GFP internalization observed by confocal microscopy using the INCell Analyzer 3000 indicated that within 5 to 10 min of stimulation by the agonist, I-TAC, small pits/vesicles approximately 1 μm in size are seen accumulating in the cytoplasm. Following longer incubations with agonist (30 min to 3 h), these small vesicles become less evident and a more prominent single, large, perinuclear vesicle (late endosome/lysosome) develops (Fig. 4). The size of the smaller vesicles is close to the resolution limit of the microscope ($\sim$0.6 μm), which also vary significantly

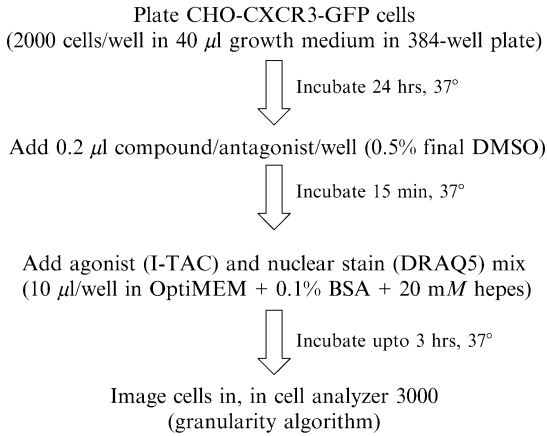

FIG. 2. Assay protocol for CXCR3-GFP receptor internalization assay.

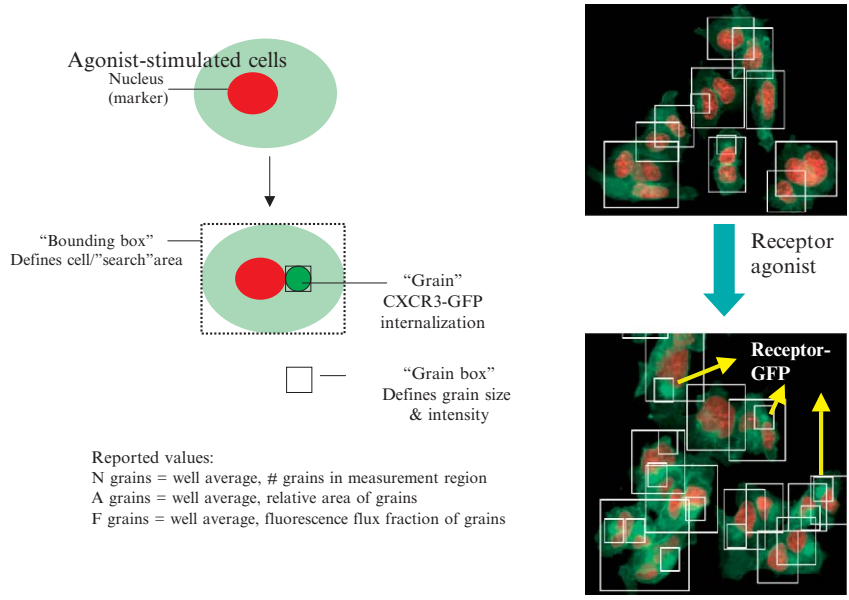

FIG. 3. Granularity analysis algorithm for CXCR3-GFP internalization assay.

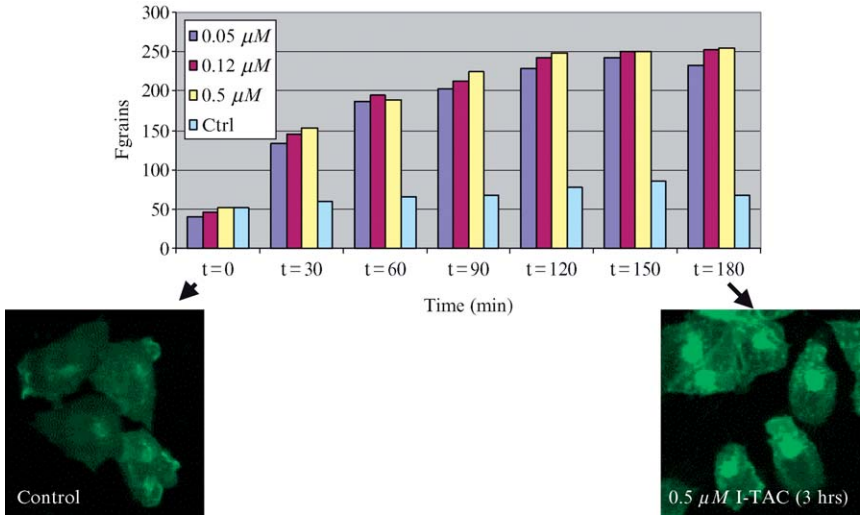

FIG. 4. Time course of agonist-induced CXCR3-GFP receptor internalization. CHO cells stably expressing CXCR3-GFP were stimulated with various (0, 0.05, 0.12, and 0.5 μM) concentrations of the agonist I-TAC and assayed as described for 0 to 180 min. Results are expressed as Fgrains based on granularity analysis algorithm as shown in Fig. 3. Confocal images from INCell 3000 are shown for control cells (no agonist stimulation) and for cells stimulated with 0.5 μM I-TAC for 3 h.

in number and size from cell to cell. Hence, larger vesicles are more practical to measure and quantitate.

Similar to the time course of agonist stimulation, the response (receptor trafficking from the plasma membrane to intracellular vesicle) is also dose dependent, as quantified in Fig. 5. Importantly, the dose-dependent response is inhibited in the presence of the receptor antagonist. The receptor trafficking assay monitored by receptor-GFP exhibits comparable sensitivity to other GPCR assays (Fig. 6).

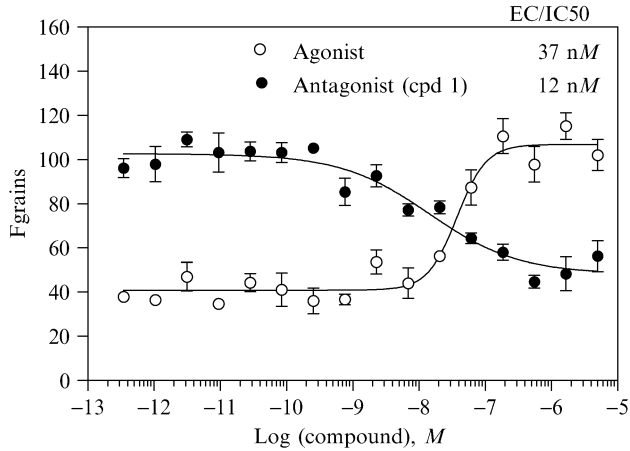

FIG. 5. Agonist and antagonist dose responses in CXCR3-GFP receptor internalization assay. Receptor internalization assays with CHO cells stably expressing CXCR3-GFP were conducted as described using various concentrations of the agonist I-TAC or various concentrations of an antagonist in the presence of 0.5 μM I-TAC (EC_{90}). Images were acquired and data quantified as described previously.

	IC50 (n*M*)			
Sample	Receptor binding (n*M*)	BLA (n*M*)	FLIPR (n*M*)	IN cell (n*M*)
Compound 2	640	462	196	510
Compound 3	690	271	269	540
Compound 4	520	289	173	607
Compound 5	1240	396	564	342
Compound 6	1800	981	206	1957
Compound 7	>50% inhibition @ 10 μM	113	43	250

FIG. 6. Comparison of assay sensitivity for the CXCR3 receptor. IC_{50} values of six compounds were compared among receptor binding, reporter gene β-lactamase assay, second messenger Ca^{2+} assay measured by FLIPR, and the receptor internalization assay (INCell) for the CXCR3 receptor.

Monitoring GPCR Trafficking via Receptor–Arrestin–GFP

Overview

An indirect method to measure GPCR activation using localization of an arrestin–GFP chimera was initially developed by Norak Biosciences and commercialized as the Transfluor assay. In this assay, the arrestin–GFP fluorescence is localized in the cytoplasm as a diffuse signal when receptors are inactive at the plasma membrane and, upon receptor activation, the arrestin–GFP first translocates to the activated receptors at the plasma membrane and is subsequently internalized into small pits near the plasma membrane (as seen with the MRG-X1 receptor, case I described later) or larger vesicles (as seen with the NK1 receptor, case II described later) based on the affinity of the arrestin for the activated and phosphorylated receptor (Oakley *et al.*, 2002) (Figs. 1 and 7). An advantage of the Transfluor assay is that it does not require manipulation of the receptor sequence.

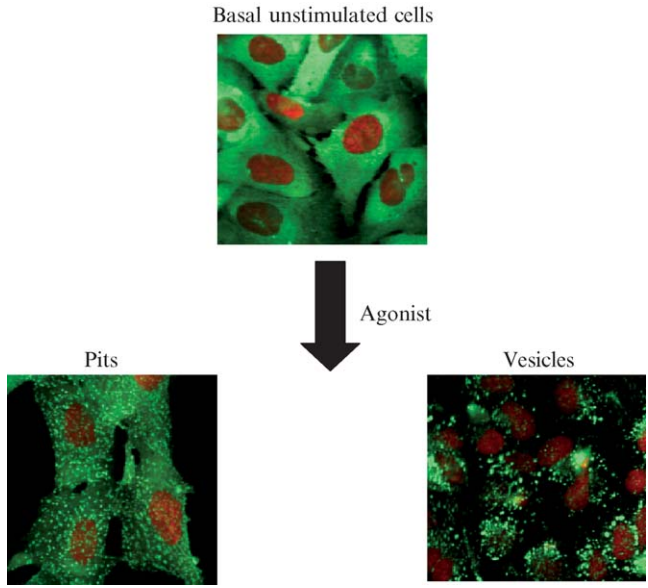

FIG. 7. Cellular phenotypes observed in Transfluor assay. Example cellular images of basal unstimulated cells, cells exhibiting small pits near the surface of the plasma membrane, and cells exhibiting larger internal vesicles upon agonist stimulation are shown.

Case I: MRG-X1 Receptor

Assay Protocol

U2OS-hMRGX1-βarrGFP stable cells are cultured in MEM supplemented with 10% heat-inactivated fetal bovine serum, 4 m*M* L-glutamine, 10 μg/ml gentamicin, 10 m*M* HEPES, 0.4 mg/ml G-418, and 0.4 mg/ml Zeocin. The assay protocol for an antagonist screen is shown in Fig. 8. Confocal microscopy is performed on the INCell Analyzer 3000 (GE Healthcare, Piscataway, NJ) using the granularity analysis and toxicity algorithms as shown in Fig. 9.

Data Analysis

In the INCell Analyzer 3000 imager, two excitation lines, 488 and 633 nm, are used to simultaneously excite β-arrestin–GFP and the DRAQ5 nuclear stain, respectively. Confocal images from the INCell 3000 are analyzed by the Raven software. Images of 200–300 cells from each well are captured and analyzed with the granularity analysis algorithm using the Raven software of IN Cell Analyzer 3000. Individual cells or nuclei are first identified by thresholding the red channel (DRAQ5). From the nucleus,

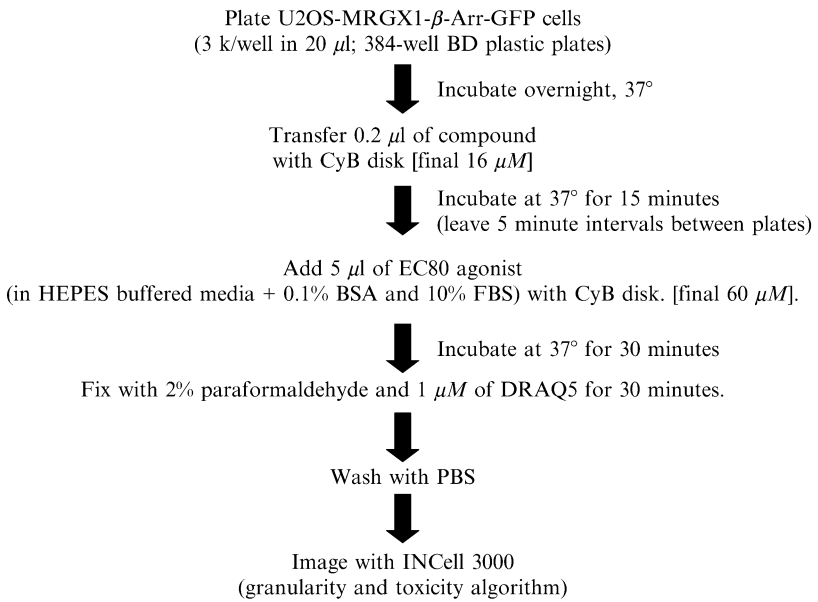

FIG. 8. Transfluor assay protocol for MRG-X1 receptor internalization assay.

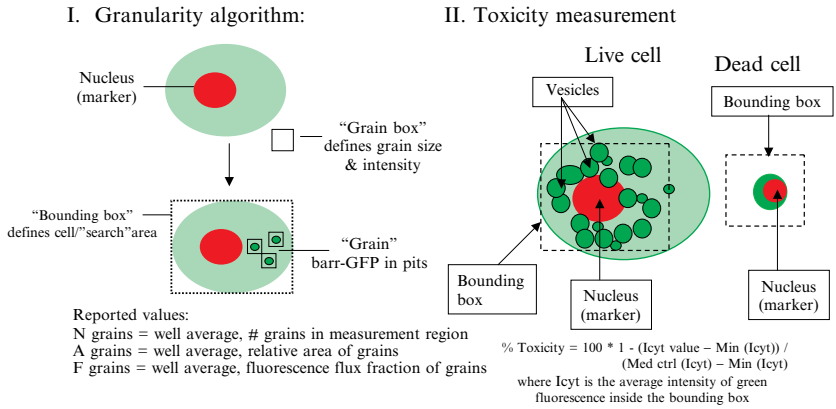

FIG. 9. Schematic representation of granularity and toxicity algorithms for the Transfluor receptor internalization assay.

a rectangular bounding box is dilated out to the edge of the cell with a dilation setting of 15 pixels. Within this bounding box, fluorescent spots of β-arrestin–GFP distribution are identified and outlined using an intensity gradient of 1.2 and a grain size of 4 pixels (Fig. 9). This granularity analysis algorithm is used to measure the number of fluorescent spots (Fgrains) based on fluorescent intensity and size of the grains, and the average value from all the cells in a well is used to obtain the ''Fgrain'' value for the well. The same granularity analysis algorithm is used to measure potential toxicity introduced by compounds based on the cellular morphology. The Icyt value is used to measure the average intensity of the green fluorescence inside the bounding box. Low Icyt values may indicate toxicity (resulting in either cell lysis or cells rounding up) displaying little or no GFP distribution in the cytoplasm and the plasma membrane, whereas high Icyt values may be due to the presence of a fluorescent compound.

Assay Characterization

INCell3000 analysis of MRG-X1 receptor trafficking indicates that in basal conditions, the β-arrestin–GFP fluorescence appears to be located primarily in the cytoplasm. Upon stimulation with increasing concentrations of the agonist BAM15, there is a corresponding increase in the punctate ''pit'' staining within the cell (Fig. 10). Agonist addition induces visible receptor internalization beginning from 1 μM BAM15 and is maximal at 100 μM BAM15. The receptor internalization quantified with the granularity analysis algorithm exhibits an EC_{50} of $\sim$14 μM (Fig. 10). Kinetics of receptor internalization indicates that this process plateaus

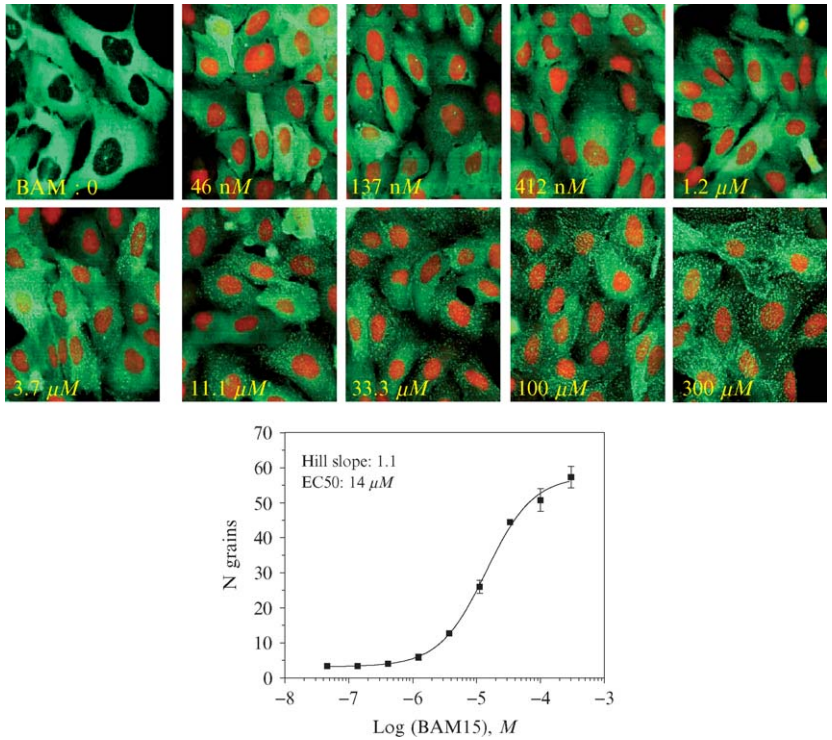

FIG. 10. Dose response of agonist-induced MRG-X1 receptor internalization. U2OS-MRGX1–βarr–GFP cells were assayed as described previously. Sample images from INCell 3000 (top) at increasing concentrations of the agonist BAM15 and a dose–response curve derived from processed data (bottom) are shown. Reprinted from Kunapuli, P., Lee, S., Zheng, W., Alberts, M., Kornienko, O., Mull, R., Kreamer, A., Hwang, J.-I., Simon, M. I., and Strulovici, B. Identification of small molecule antagonists of the human mass-related gene (MRG)-×1 receptor. *Anal. Biochem.* **351,** 50–61. Copyright (2006), with permission from Elsevier.

10 min after initiation of receptor stimulation and is stable for 60 min (Fig. 11).

Interestingly, the EC_{50} of the agonist response in the receptor-trafficking assay (14 μM) appears to be significantly right shifted compared to the BLA (55 nM) and second messenger FLIPR (8 nM) assays for the MRG-X1 receptor. However, it is important to bear in mind some key differentiating features in these assays, such as the cellular background (U2OS vs CHO), method of clone selection (traditional cloning vs single cell FACS based on functional response), and relationship to cellular signaling (receptor internalization is independent of cellular signaling, unlike the BLA or FLIPR assays). The lack of correlation between the agonist EC_{50} in the receptor-trafficking assay and the second messenger assay appears to be unique for this receptor and is

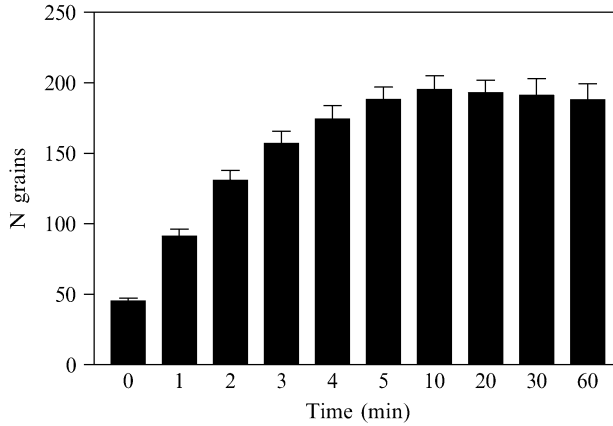

FIG. 11. Time course of receptor internalization for MRGX1 receptors in the Transfluor assay. U2OS-MRGX1–βarr–GFP cells were assayed as described with 0.3 m*M* BAM15 for 30 min at 37°. Data were processed as described previously. Reprinted from Kunapuli, P., Lee, S., Zheng, W., Alberts, M., Kornienko, O., Mull, R., Kreamer, A., Hwang, J.-I., Simon, M. I., and Strulovici, B. Identification of small molecule antagonists of the human mass-related gene (MRG)-×1 receptor. *Anal. Biochem.* **351,** 50–61. Copyright (2006), with permission from Elsevier.

exhibited by three different clones. This phenomenon has not been observed for other GPCRs (Howell, Lee, and Kunapuli, personal communication).

Assay Application

The MRG-X1 receptor-trafficking assay, monitored by β-arrestin–GFP, is used as a secondary/follow-up assay after HTS for MRG-X1 receptor antagonists using the BLA assay. In the absence of a suitable radioligand for a high-throughput receptor-binding assay using membranes from CHO-MRG-X1-BLA cells, the compounds identified from the primary screen are analyzed further for their ability to inhibit agonist-induced receptor internalization using the proximal, high-content assay. Consistent with the lower sensitivity of the receptor-trafficking assay as seen with BAM15, the IC_{50} of most compounds in this assay is right shifted compared to the BLA, FLIPR, or binding assays. In the presence of 10 μM concentration of each of these compounds and 60 μM BAM15 (EC_{80} concentration for receptor-trafficking assay), the cellular phenotype appears comparable to the basal, unstimulated state, with β-arrestin–GFP exhibiting diffuse cytoplasmic staining, implicating an uncoupled state from the receptor . The IC_{50} of some of these compounds is shown in Fig. 12. However, despite a lower assay sensitivity compared to the other functional assays, this high-content assay proved to be useful in assessing compound toxicity, which is often a common issue in cell-based assays. For example, in Fig. 13A, the sample

	IC50 (n*M*)			
Sample #	BLA	FLIPR	InCell	Binding
8	50	103	730	320
9	64	157	2800	ND
10	80	187	550	182
11	90	209	6782	ND
12	124	904	2200	1220
13	140	751	3600	607
14	163	220	2200	1430
15	165	334	4800	630
16	200	1500	5200	ND
17	209	492	10,000	ND
18	244	460	5200	1290
19	252	3300	8800	2400
20	290	1300	6300	1850
21	375	2700	29,000	1180
22	418	9800	13,500	2510
23	556	632	5600	1850

FIG. 12. Dose response for MRG-X1 receptor antagonist. The MRGX1 receptor internalization assay was performed as described. Cellular images from INCell 3000 confocal microscope (left) were analyzed with the granularity analysis algorithm (exhibited as percentage inhibition of 80 μM BAM15-induced signal) and toxicity algorithms (right) for compound exhibiting minimal toxicity (A) and compound exhibiting 66% toxicity at 80 μM (B). Reprinted from Kunapuli, P., Lee, S., Zheng, W., Alberts, M., Kornienko, O., Mull, R., Kreamer, A., Hwang, J.-I., Simon, M. I., and Strulovici, B. Identification of small molecule antagonists of the human mass-related gene (MRG)-×1 receptor. *Anal. Biochem.* **351,** 50–61. Copyright (2006), with permission from Elsevier.

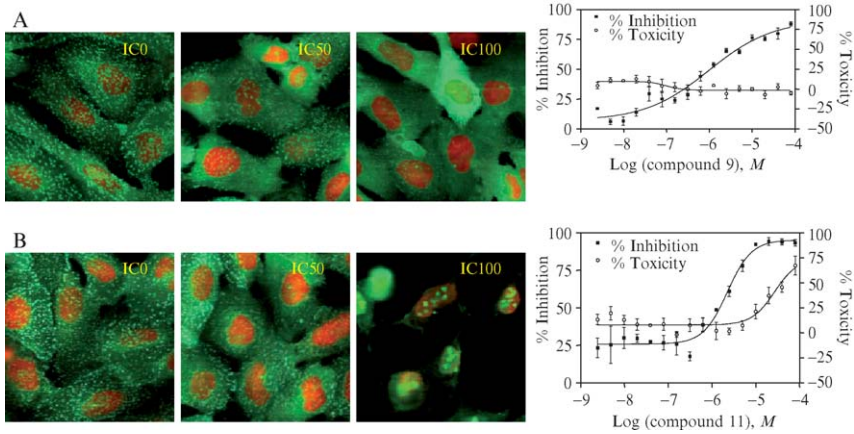

FIG. 13. Comparison of assay sensitivities for the MRG-X1 receptor. IC_{50} values of 16 compounds were compared among reporter gene β-lactamase assay, second messenger Ca^{2+} assay measured by FLIPR, receptor internalization assay, and whole cell receptor-binding assay for the MRG-X1 receptor.

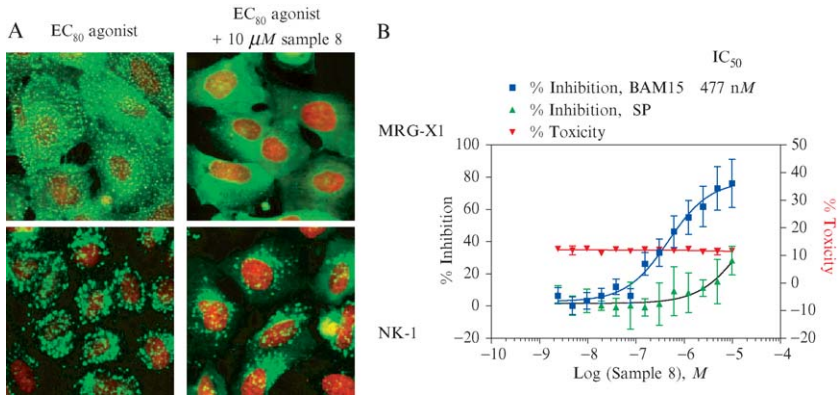

FIG. 14. Specificity analysis. The Transfluor assay was performed as described to determine the specificity of MRG-X1 antagonist for the MRG-X1 receptors. (A) Sample confocal images from INCell 3000 and (B) a dose–response curve of an MRG-X1 receptor antagonist are shown. Reprinted from Kunapuli, P., Lee, S., Zheng, W., Alberts, M., Kornienko, O., Mull, R., Kreamer, A., Hwang, J.-I., Simon, M. I., and Strulovici, B. Identification of small molecule antagonists of the human mass-related gene (MRG)-×1 receptor. *Anal. Biochem.* **351,** 50–61. Copyright (2006), with permission from Elsevier.

exhibits minimal (if any) toxicity even at 100 μM, as measured by a cell morphology-based toxicity algorithm, whereas in Fig. 13B, there is higher toxicity exhibited by the compound. In addition, some of these compounds were also tested against an unrelated class A GPCR, the neurokinin NK1 receptor, in a similar receptor-trafficking assay using U2OS-neurokinin receptor 1–β-arrestin–GFP cells. Most of these compounds were inactive or weak in inhibiting substance P-induced NK1 receptor internalization (Fig. 14), demonstrating specificity of the assay.

Case Study 2: NK1 Receptor Trafficking

Overview

The NK1–β-arrestin–GFP receptor internalization assay was used as a follow-up/hit funneling strategy for several thousand compounds originating from primary HTS using the BLA assay. The Transfluor assay was established in a semiautomated mode with various instruments for liquid handling. The granularity analysis and toxicity algorithms used for this analysis are similar to those described for the MRG-X1 Transfluor assay.

Assay Protocol

The Transfluor assay protocol for the U2OS-NK1–βarr–GFP cells in a semiautomated format is described in Fig. 15.

Assay Characterization

The kinetics of receptor internalization in U2OS-NK1–βarr–GFP cells upon stimulation with the agonist, substance P (SP), reveals that this process plateaus at ~45 min after receptor stimulation (Fig. 16). These cells appear to be tolerant to ~1% dimethyl sulfoxide (DMSO), an important parameter for compound screening (Fig. 17A). The assay appears tolerant to cell densities ranging from 2000 to 4000 cells/well, resulting in comparable responses with respect to assay window and assay sensitivity,

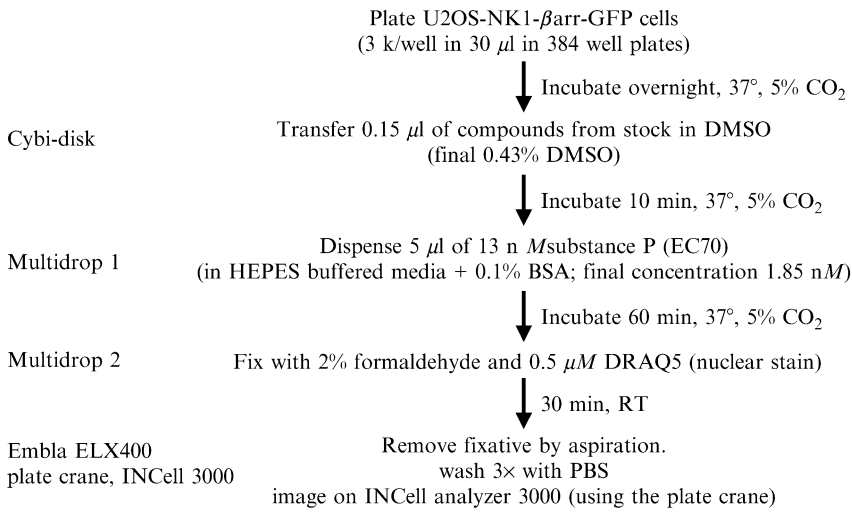

FIG. 15. Transfluor assay protocol for NK1 receptor internalization assay.

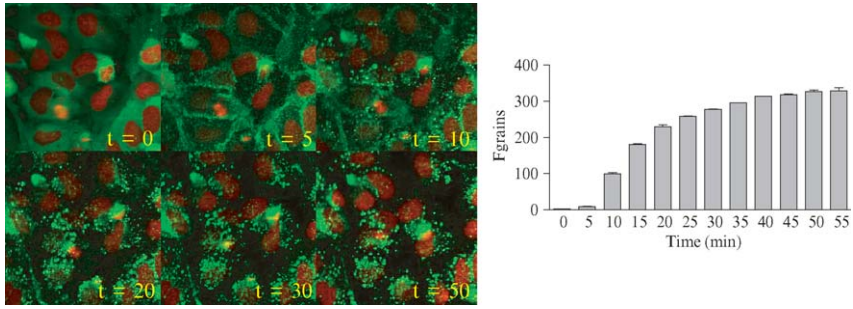

FIG. 16. Kinetics of NK1 receptor internalization. The NK1 Transfluor assay was conducted as described with 0.5 μM substance P (measured in Fgrains or relative grain intensity). Images taken at 0, 5, 10, 20, 30, and 50 min are shown.

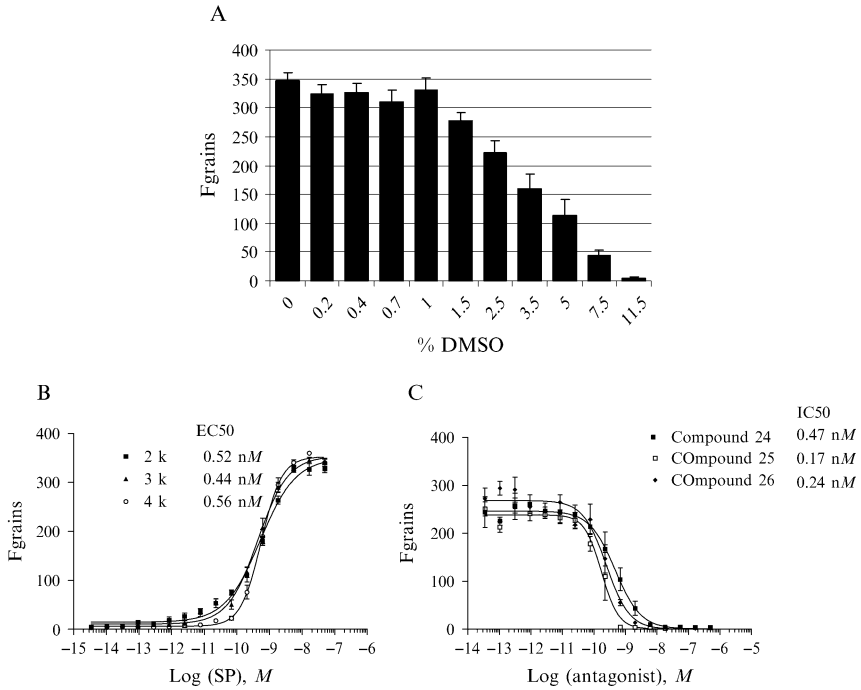

FIG. 17. Assay characteristics of the NK1 Transfluor assay. The NK1 Transfluor assay was conducted as described in the presence of various concentrations of DMSO and 0.5 μM substance P (A), in the presence of various cell densities and various concentrations of substance P (B), and in the presence of various concentrations of receptor antagonists with 0.5 μM substance P (C). The response was measured in Fgrains.

exhibiting an EC_{50} of 0.5 nM for SP (Fig. 17B). More importantly, receptor pharmacology (Fig. 17C) with known antagonists was also comparable for three compounds in this assay (and between second messenger and reporter gene assays, data not shown).

Screening

Whole plate assays using U2OS-NK1–βarr–GFP cells in the Transfluor assay show acceptable S/N and plate CVs (~6%) for screening (Fig. 18A). The assay plate format used for the follow-up screen of ~3000 compounds in triplicate at two concentrations (8.5 and 2.1 μM, starting from 2 mM and 0.5 μM samples, respectively) is shown in Fig. 18C. Each of the assay steps was set up at a different instrument workstation (CyB Disk, Multidrop 1 and 2, ELX-405 and plate crane for the INCell 3000 as shown in Fig. 15).

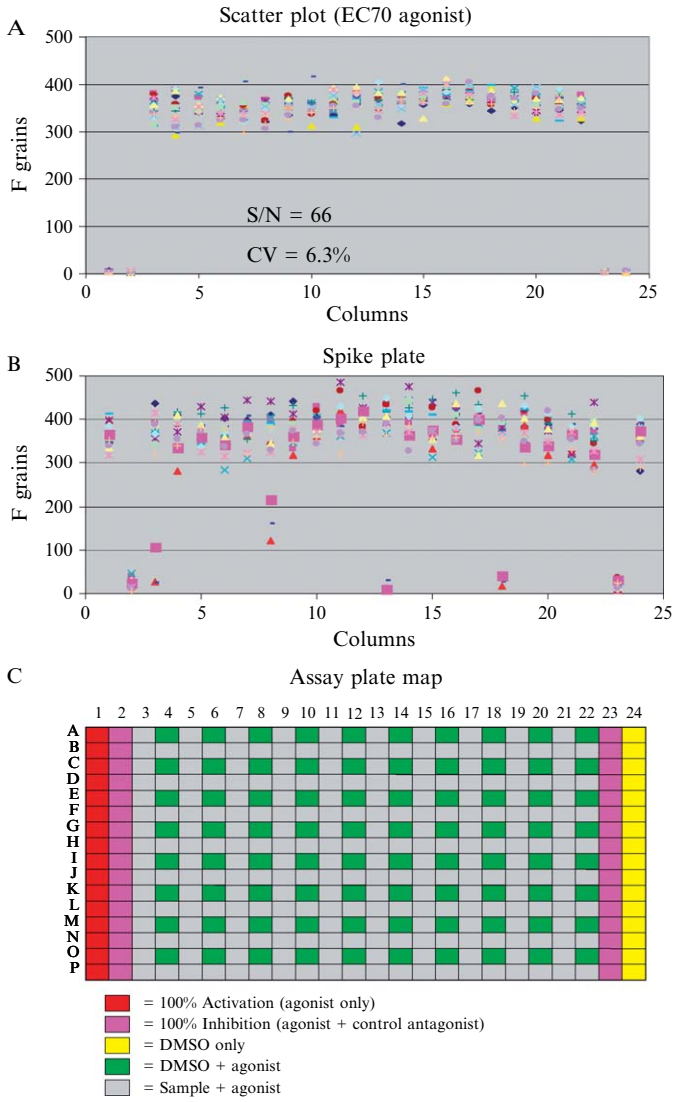

FIG. 18. Whole plate assay for NK1 receptor antagonists. (A) The whole plate assay with DMSO reveals acceptable S/N and plate CV (~6%). The DMSO plate contained the NK1 receptor antagonist compound 25 in columns 1 and 2 and basal unstimulated cells in columns 23 and 24. Columns 1–22 were stimulated with 1.85 n*M* substance P. (B) The plate map of the spiked plate is similar to the plate map for the screen, with the exception that most wells between columns 3 and 22 contained DMSO. Some random wells were spiked with compound 25 at IC_{50}, IC_{70}, or IC_{100}. (C) Schematic plate map for assay plates in the screen. Column 1 was used for 100% activation with only agonist addition. Columns 2 and 23 were treated with

Compound stock concentration	2 mM	500 μM
Final compound concentration	8.5 μM	2.1 μM
# of compounds screened	2877	2877
Median > 30% inhibition	925 (32.2%)	336 (11.7%)
Toxic compounds	192 (20.8% of hits)	13 (3.9% of hits)
Fluorescent compounds	4 (0.4% of hits)	4 (1.2% of hits)
False positives (nonsample areas)	20 (2.2%)	0
Total actives in transfluor assay	709	319

FIG. 19. Screen summary. A total of 2877 compounds were screened in 384-well format at 8.5 and 2.1 μM concentrations in triplicate. Toxic compounds (based on cellular image and toxicity algorithm) were eliminated by visualizing the images of all of the hits.

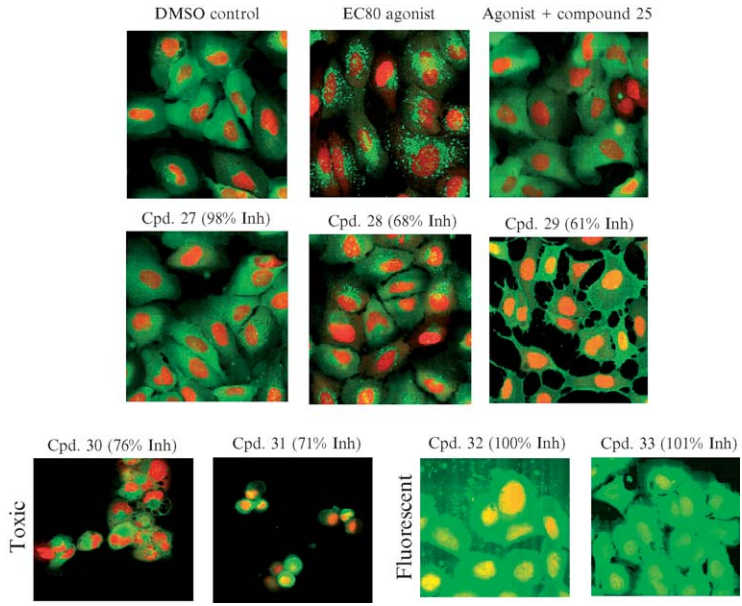

FIG. 20. Cellular phenotypes from NK1 antagonist screen. Example images of the cellular phenotype from the NK1 receptor antagonist screen using the Transfluor assay are shown.

agonist (1.85 nM final concentration of substance P) and compound 25 for 100% inhibition control. Column 24 was treated with DMSO and agonist. Quadrants 1, 3, and 4 were treated with sample compounds and agonist, while quadrant 2 was treated with DMSO as a control and agonist. Data were processed as described earlier.

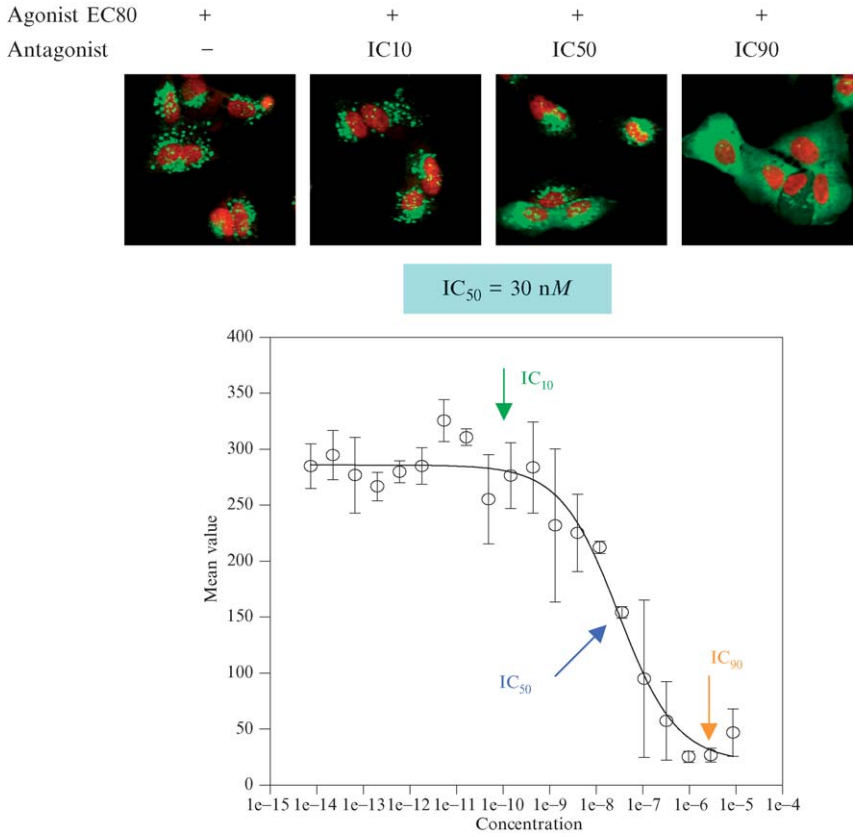

FIG. 21. Example compound dose response. Sample images (top) of compound 34 at IC_{10}, IC_{50}, and IC_{90} are shown with β-arrestion–GFP in the green channel and DRAQ5 in the red channel, and a IC_{50} curve of a 20-point titration (bottom) is shown for compound 24.

The assay took a total of ~6 h to complete for ~3000 compounds in triplicate at two compound concentrations. The image size for acquisition in INCell 3000 was set to 0.75 × 0.375 mm for two color channels: green for GFP and red for DRAQ5. The minimum cell count was set to 50 cells/well. The live image analysis took a total of 10.5 h to complete for all the assay plates. The images were analyzed by the granularity analysis algorithm. Fgrains refer to the fraction of cellular fluorescence present in the qualifying grains. Results from this screen are shown in Fig. 19, and sample images from different wells are shown in Fig. 20.

Among the confirmed compounds in the Transfluor assay, dose responses were performed for 72 compounds. An example titration with

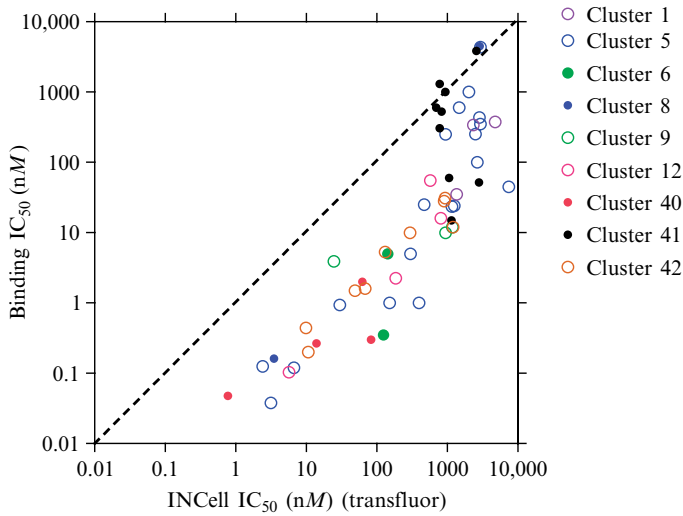

FIG. 22. Correlation plot for NK1 receptor antagonists: Comparison of the IC_{50} in the receptor binding and Transfluor assays among 72 NK1 receptor antagonists. IC_{50} values obtained from the INCell 3000 (TransFluor assay) are on the *x* axis, and IC_{50} values from binding data are plotted on the *y* axis. The compounds were clustered by their structure. Data based on Fgrain measurements using granularity algorithm v001.

corresponding cellular images is shown in Fig. 21. The IC_{50} values obtained were directly compared to those from receptor-binding experiments. Although there appeared to be a rightward shift in IC_{50} values from the Transfluor assay for these compounds, there was reasonable correlation with the binding data as shown in Fig. 22. Possible explanations for the rightward shift in the Transfluor assay could be due to differences in the assay protocol (e.g., Transfluor assay used 1.85 n*M* SP vs 0.1 n*M* SP in binding assay). In addition, in the binding assay, the compounds were preincubated with the cells for at least 30 min before agonist addition, thereby increasing the assay sensitivity for weak binders. Interestingly, for some of the compounds (e.g., cluster # 41), there is a better correlation between the receptor binding and Transfluor assays than others (e.g., cluster #6 and #40).

Acknowledgments

We thank Lin-Lin Shiao and Dr. Kathleen Sullivan for the CXCR3-GFP cell line. We are also grateful to Kevin Nguyen for his help in preparing the compound plates for dose–response studies and to Dr. James Inglese (current address: National Institutes of Health, MD) for valuable suggestions during the course of this work.

References

Bleicher, K. H. (2003). Hit and lead generation: Beyond high-throughput screening. *Nature Rev. Drug Disc.* **2,** 369–378.

Civelli, O., Nothacker, H. P., Saito, Y., Wang, Z., Lin, S. H. S., and Reinscheid, R. K. (2001). Novel neurotransmitters as natural ligands of orphan G-protein-coupled receptors. *Trends Neurosci.* **24,** 230–237.

Drews, J. (2000). Drug discovery: A historical perspective. *Science* **287,** 1960–1964.

Ferguson, S. S. (2001). Evolving concepts in G protein-coupled receptor endocytosis: The role in receptor desensitization and signaling. *Pharmacol. Rev.* **53,** 1–24.

Gautam, N., Downes, G. B., Yan, K., and Kisselev, O. (1998). The G protein bg complex. *Cell Signal* **10,** 447–455.

Gilman, A. G. (1987). G proteins: Transducers of receptor generated signals. *Annu Rev. Biochem.* **56,** 615–649.

Goodman, O. B., Jr., Krupnick, J. G., Santini, F., Gurevich, V. V., Penn, R. B., Gagnon, A. W., Keen, J. H., and Benovic, J. L. (1996). β-arrestin acts as a clathrin adaptor in endocytosis of the β2-adrenergic receptor. *Nature* **383,** 447–450.

Gurevich, V. V., Dion, S. B., Onorato, J. J., Ptasienski, J., Kim, C. M., Sterne-Marr, R., Hosey, M. M., and Benovic, J. L. (1995). Arrestin interactions with G protein-coupled receptors: Direct binding studies of wild type and mutant arrestins with rhodopsin, β2-adrenergic and M2 muscarinic cholinergic receptors. *J. Biol. Chem.* **270,** 720–731.

Hopkins, A. L., and Groom, C. R. (2002). The druggable genome. *Nature Rev. Drug Disc.* **1,** 727–730.

Krupnick, J. G., Goodman, O. B., Jr., Keen, J. H., and Benovic, J. L. (1997). Arrestin/clathrin interaction: Localizatin of the clathrin binding domain of non visual arrestins to the carboxy terminus. *J. Biol. Chem.* **272,** 15011–15016.

Krupnick, J. G., and Benovic, J. L. (1998). The role of receptor kinases and arrestins in G protein-coupled receptor regulation. *Annu. Rev. Pharmacol. Toxicol.* **38,** 289–319.

Lefkowitz, R. J. (1993). G protein-coupled receptor kinases. *Cell* **74,** 409–412.

Marchese, A., George, S. R., Kolalowski, L. F., Jr., Lynch, K. R., and O'Dowd, B. F. (1999). Novel GPCRs and their endogenous ligands: Expanding the boundaries of physiology and pharmacology. *Trends Pharmacol. Sci.* **20,** 370–375.

Neer, E. J. (1995). Heterotrimeric G proteins: Organizers of transmembrane signals. *Cell* **80,** 249–257.

Oakley, R. H., Hudson, C. C., Cruickshank, R. D., Meyers, D. M., Payne, R. E., Jr., Rhem, S. M., and Loomis, C. R. (2002). The cellular distribution of fluorescently labeled arrestins provides a robust, sensitive and universal assay for screening G protein-coupled receptors. *Assay Drug Dev. Tech.* **1,** 21–30.

Oakley, R. H., Laporte, S. A., Holt, J. A., Barak, L. S., and Caron, M. G. (1999). Association of beta-arrestin with G protein-coupled receptors during clathrin-mediated endocytosis dictates the profile of receptor resensitization. *J. Biol. Chem.* **274,** 32248–32257.

Oakley, R. H., Laporte, S. A., Holt, J. A., Barak, L. S., and Caron, M. G. (2001). Molecular determinants underlying the formation of stable intracellular G protein-coupled receptor-beta-arrestin complexes after receptor endocytosis. *J. Biol. Chem.* **276,** 19452–19460.

Oakley, R. H., Laporte, S. A., Holt, J. A., Caron, M. G., and Barak, L. S. (2000). Differential affinities of visual arrestin, beta arrestin 1, and beta arrestin 2 for G protein-coupled receptors delineate two major classes of receptors. *J. Biol. Chem.* **275,** 17201–17210.

Sterne-Marr, R., and Benovic, J. L. (1995). Regulation of G protein-coupled receptors by receptor kinases and arrestins. *Vitam. Horm.* **51,** 193–234.